

# Polarization of the Cosmic Microwave Background Radiation

Yasin Memari, March 2007

The CMB radiation is completely characterized by its temperature anisotropy and polarization in each direction in the sky. Today, studies of the temperature anisotropies in the CMB have provided strong constraints on many of the cosmological parameters. However, for precision cosmology we still need to consider the polarization information of the CMB to break some of the degeneracies that exist between some combinations of parameters. Furthermore, the additional information from CMB polarization is very helpful for studies of cosmological physics on super-horizon scales, where our ability of extracting cosmological information is limited by cosmic variance. Moreover, polarization data can help to distinguish the ingredients which go to make up the temperature power spectrum and therefore the cosmological model. We know that different modes of temperature anisotropies (scalar, vector and tensor) give distinguishable polarization patterns. On the other hand, polarization provides us with a direct probe of the last scattering surface, as opposed to the temperature anisotropies that are affected by various physical effects that occur between the last scattering surface and present. Therefore polarization can help distinguish the sources of anisotropy. However, The CMB polarization is extremely difficult to measure, because it is small and because the polarized foregrounds are poorly known. Nevertheless, there are a number of upcoming experiments designed to make such measurements.

## 1 The Origin of CMB Polarization

The CMB polarization originates from re-scattering of the primordial photons on the hot electron gas on their way to us. Imagine an electron at rest in the origin. This electron is accelerated by an incoming plane wave of radiation with wave vector  $\vec{k}_i$  and re-radiates an outgoing wave along  $\vec{k}_s$ . Compton scattering allows all the radiation transverse to the outgoing direction to pass through unimpeded, while stopping any radiation parallel to the outgoing direction. Such a process in which the photon energy remain unchanged is called Thomson scattering. The plane spanned by  $\vec{k}_i$  and  $\vec{k}_s$  is the scattering plane, and the cross-section for outgoing photons is proportional to  $|\hat{k}_i \cdot \hat{k}_s|^2$ . Thus the scattered radiation intensity peaks in the direction normal to the incident polarization.

Now imagine the incoming plane wave is travelling along the  $x$  axis towards the origin, with its corresponding electric and magnetic fields oscillating in the  $y$ - $z$  plane. If the intensity along the two transverse directions  $y$  and  $z$  is equal, then the light is unpolarized. This ray then scatters off an electron at the origin and gets deflected into all directions with varying probability. The Thomson scattering can then guarantee that the outgoing radiation observed in the  $+\hat{z}$  direction has a linear polarization pattern. This is due to the fact that none of the incoming intensity along the outgoing direction ( $z$ -axis) gets transmitted. The intensity along the  $y$ -axis is the only component of the polarization that passes through unimpeded in the  $+\hat{z}$  direction. Hence the outgoing radiation is polarized in the  $y$ -direction if observed along the  $z$  axis. Obviously, this result is for one single incoming ray and if we generalize to radiation incident from all directions we realise that producing polarization will not be as easy.

Imagine an unpolarized incoming isotropic radiation (monopole) incident from all directions on an electron. Figure 1 is a simple representation of such a case where incoming rays from only two directions, the  $+\hat{x}$  and  $+\hat{y}$  directions, have been depicted. We are still interested in the polarization of outgoing photons in the  $\hat{z}$  direction. The intensity of the outgoing ray along the  $x$ -axis comes from the radiation incident from the  $\hat{y}$  direction, while the outgoing  $y$ -intensity comes from the radiation from the  $x$ -axis. Since the incoming amplitudes from both directions have equal intensity for an isotropic radiation, the outgoing radiation along the  $x$  and  $y$  axes will turn out to have equal intensities, leading to an unpolarized outgoing radiation along the  $\hat{z}$  direction. Hence, isotropic radiation does not produce polarization.

Incoming dipole radiation also produces no polarization. The simplest example of a dipole is the case when the incoming radiation is hotter (colder) than average from the  $+\hat{x}$  ( $+\hat{y}$ ) direction and colder than average from  $-\hat{x}$  ( $-\hat{y}$ ) direction. Figure 1 represent such a case. Here the outgoing intensity along the  $x$ -axis comes from the  $\pm\hat{y}$  incident radiations which have the average temperature. The two rays from the  $\pm\hat{x}$  directions also produce an outgoing intensity that is neither hot nor cold along the  $y$  - axis because it is just equal to the average intensity of the incoming rays in along the  $\pm\hat{x}$  direction. Since these have the same average intensity the intensity of the outgoing wave along  $x$  and  $y$  axes are equal. Hence the net result is outgoing unpolarized radiation.

To produce polarized radiation, the incident radiation field should actually possess a quadrupole variation in intensity or temperature. This happens when the average incoming radiation from the  $\hat{y}$

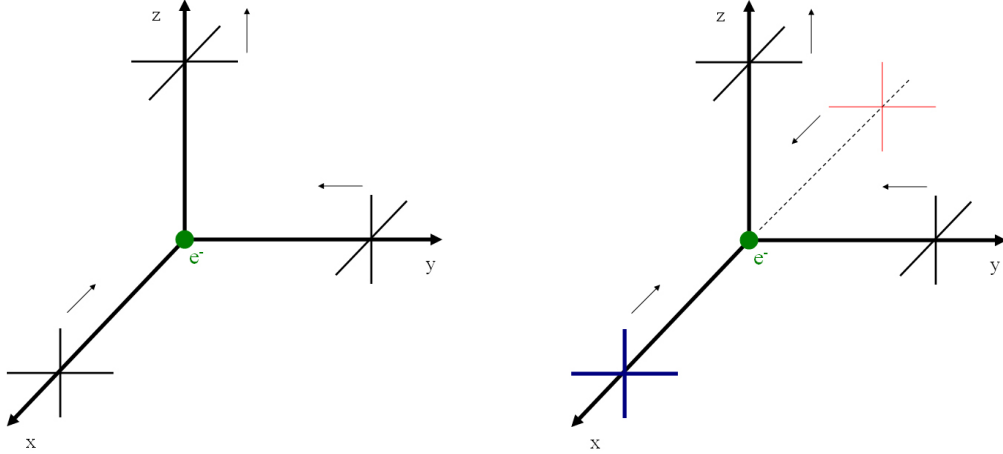


Figure 1: Thomson scattering of incoming isotropic (left) and dipole (right) radiation. Here black lines denote radiation with average intensity. Blue (thick) lines show incoming radiation that is hotter than average intensity and red (thin) lines represent radiation that is colder than average. The net result for both isotropic and dipole radiation is outgoing unpolarized light.

direction is hotter (colder) than it is along the  $\hat{x}$  direction. Figure 2 illustrates such a case where the incident radiation along the  $x$ -axis is hotter than it is in the  $y$  direction. Therefore, the intensity of the outgoing radiation is greater along the  $y$ -axis than along the  $x$ -axis. Thus, the outgoing radiation is polarized for a quadrupole radiation. Furthermore, since the scattering cross-section of the Thomson scattering is quadratic, we do not proceed to study the effect of larger multipoles.

In reality, a quadrupole anisotropy of the photon flux at one point on the last scattering surface, when the universe is still ionized, can generate polarization in the cosmic background radiation. Before recombination, the high electron density means that the mean free path of the photons is too small to produce a quadrupole; however after the recombination the electron density is too low for significant Thomson scattering to occur. The polarization can only be produced during a short period around recombination, so we expect the amplitude of the polarization to be smaller than the temperature anisotropies. Also, although late re-ionization, which is due to the process of early star formation, enhances the polarization at large scales, it does not modify the quantitative conclusion that the polarization signal is expected to be small.

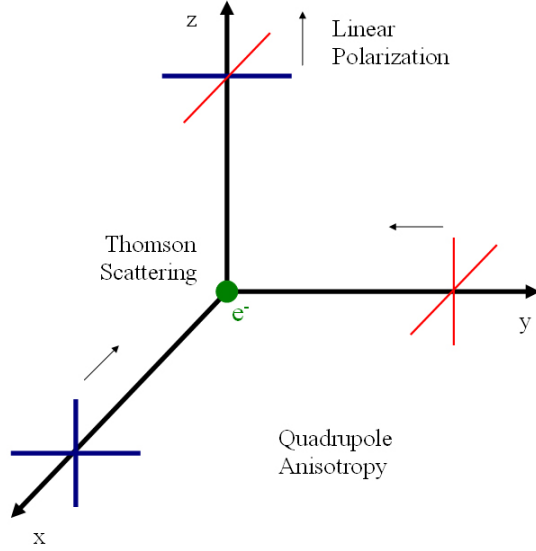


Figure 2: Thomson scattering of radiation with a quadrupole anisotropy generates linear polarization. Blue colors (thick lines) represent hot and red colors (thin lines) cold radiation.

The quadrupole anisotropy of the photon flux in the last scattering epoch can arise from the velocity gradients of the density fluctuations. In the photon-baryon fluid rest frame, the fluid is accelerated towards the cold spot, or decelerated towards a hot spot. In the former case, the velocity of neighboring particles tends to diverge radially from and converge transversely to the scattering point. In the latter case, the velocity of neighboring particles tends to converge radially to and diverge transversely from the scattering point. We see the patterns produced by these processes in figure 3. Then the Doppler shift induces a quadrupole flux anisotropy around the last scattering point, leading to radial polarization in the first case and to transverse polarization in the second case. This mechanism does not produce any circular polarization, so from now we set the circular components of the polarization equal to zero.

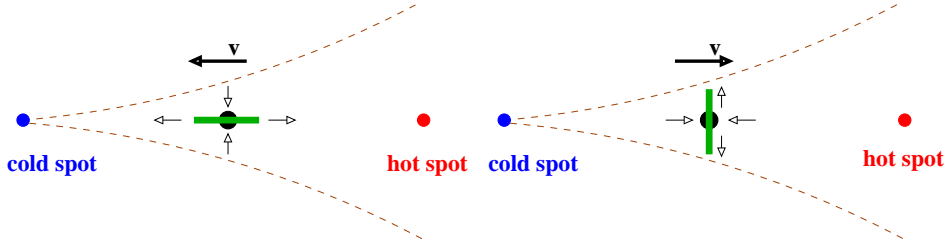


Figure 3: Generation of the local quadrupole anisotropies in the photon flux on the last scattering surface from velocity gradients.

## 2 The CMB Temperature and Polarization Fields

The temperature anisotropy of the CMB is a scalar field, so it is invariant under rotation and has zero parity (spin-0). Hence it can be expanded by the usual spherical harmonics  $Y_{lm}(\hat{n})$  on the celestial sphere

$$T(\hat{n}) = \sum_{lm} T_{lm} Y_{lm}(\hat{n}), \quad (1)$$

where  $\hat{n} = (\theta, \phi)$  is the unit vector along the line of sight. The polarization of the CMB is described by the electromagnetic field  $\vec{\epsilon}$ , which is orthogonal to its direction of propagation  $\vec{k}$ . A general radiation is an incoherent superposition of waves with the same wave vector  $\vec{k}$  and different frequencies. Choosing two basis vectors  $\hat{x}$  and  $\hat{y}$  orthogonal to  $\hat{k}$ , all statistical information is encoded in the ‘coherence matrix’  $\mathbf{C}$ :

$$\mathbf{C} = \begin{pmatrix} \langle |\vec{\epsilon}_x|^2 \rangle & \langle \vec{\epsilon}_x \vec{\epsilon}_y^* \rangle \\ \langle \vec{\epsilon}_y \vec{\epsilon}_x^* \rangle & \langle |\vec{\epsilon}_y|^2 \rangle \end{pmatrix} = \frac{1}{2} \begin{pmatrix} I + Q & U - iV \\ U + iV & I - Q \end{pmatrix},$$

where the averages are over a range of frequencies. The quantities  $I$ ,  $Q$ ,  $U$  and  $V$  are all real and called the *Stokes parameters*. The  $I$  parameter measures the radiation intensity. The other parameters describe the polarization state. It can be shown that  $I^2 \geq Q^2 + U^2 + V^2$ , and because of this property, it is always possible to decompose an observed radiation  $(I, Q, U, V)$  into two components: one completely unpolarized with  $(I - (Q^2 + U^2 + V^2)^{1/2}, 0, 0, 0)$ , and the other elliptically polarized with  $((Q^2 + U^2 + V^2)^{1/2}, Q, U, V)$ . Therefore, the parameters  $Q$  and  $U$  measure the linear polarization,

i.e. the orientation of the ellipse relative to the  $x$ -axis via the polarization angle

$$\chi = \frac{1}{2} \tan^{-1} \frac{U}{Q}, \quad (2)$$

and the polarization amplitude

$$\vec{P} = (Q^2 + U^2)^{1/2} \hat{\chi} \quad (3)$$

with  $\hat{\chi}$  representing the unit vector in the direction of the polarization. The  $Q$  and  $U$  parameters depend on the reference frame and transform like a spin-2 object, i.e. if the reference frame  $(\hat{x}, \hat{y})$  is rotated by an angle  $\psi$  around  $\hat{n}$ , then  $Q$  and  $U$  rotate to  $Q'$  and  $U'$  by an angle  $2\psi$

$$(Q \pm iU)'(\hat{n}) = e^{\mp 2i\psi} (Q \pm iU)(\hat{n}). \quad (4)$$

The fourth parameter,  $V$ , measures the relative strength of the two linear polarization states, and is nonzero only if polarization is circularly polarized.

The polarization field of the CMB can be described by the Stokes parameters  $U$  and  $Q$ . One can conveniently combine Eqns (2) and (3) into a single complex quantity representing the polarization in the direction  $\hat{n}$  on the sky

$$P(\hat{n}) = (Q + iU)(\hat{n}). \quad (5)$$

From Eqn (4) we know that this quantity is a spin-2 object, hence unlike a scalar (spin-0) function, polarization can not be expanded by the usual spherical harmonics on the surface of a sphere. The mathematical machinery necessary to represent angular distribution of the polarization of the CMB on the celestial sphere is actually the spin-weighted harmonics  ${}_s Y_{lm}(\hat{n})$ . These are a set of functions that form an orthonormal and complete basis on the sphere:

$$\int d\Omega {}_s Y_{l'm'}^*(\theta, \phi) {}_s Y_{lm}(\theta, \phi) = \delta_{l'l} \delta_{m'm}, \quad (6)$$

$$\sum_{l,m} {}_s Y_{lm}^*(\theta, \phi) {}_s Y_{lm}(\theta', \phi') = \delta(\phi - \phi') \delta(\cos \theta - \cos \theta'). \quad (7)$$

The parity relation for these functions is

$${}_s Y_{lm} \rightarrow (-1)^l {}_{-s} Y_{lm}. \quad (8)$$

There also exists a pair of raising and lowering operators,  $\bar{\partial}$  and  $\bar{\partial}$  respectively, that raise and lower the spin-weight of a function, i.e.

$$(\bar{\partial} {}_s f)' = e^{-i(s+1)\psi} (\bar{\partial} {}_s f), \quad (9)$$

$$(\bar{\partial} {}_s f)' = e^{-i(s-1)\psi} (\bar{\partial} {}_s f), \quad (10)$$

where the prime refers to a quantity in a frame rotated  $\psi$  from the original frame. The explicit form of these operators is

$$\bar{\partial} {}_s f(\theta, \phi) = -\sin^s \theta \left[ \partial_\theta + \frac{i}{\sin \theta} \partial_\phi \right] \sin^{-s} \theta {}_s f(\theta, \phi), \quad (11)$$

$$\bar{\partial} {}_s f(\theta, \phi) = -\sin^{-s} \theta \left[ \partial_\theta - \frac{i}{\sin \theta} \partial_\phi \right] \sin^s \theta {}_s f(\theta, \phi). \quad (12)$$

Using the raising and lowering operators, one can relate the spin- $s$  spherical harmonics and the usual spherical harmonics

$${}_s Y_{lm} = \left[ \frac{(l-s)!}{(l+s)!} \right]^{1/2} \bar{\partial}^s Y_{lm} \quad (13)$$

for  $0 \leq s \leq l$ , and

$${}_s Y_{lm} = \left[ \frac{(l+s)!}{(l-s)!} \right]^{1/2} (-1)^s \bar{\partial}^{-s} Y_{lm} \quad (14)$$

for  $-l \leq s \leq 0$ . Hence, using these, we can obtain

$$\pm 2 Y_{lm} = \left[ \frac{(l-s)!}{(l+s)!} \right]^{1/2} \left[ \partial_\theta^2 - \cot \theta \partial_\theta \pm \frac{2i}{\sin \theta} (\partial_\theta - \cot \theta) \partial_\phi - \frac{1}{\sin^2 \theta} \partial_\phi^2 \right] Y_{lm}. \quad (15)$$

Also, useful properties of the spin-weighted spherical harmonics are

$$\begin{aligned} {}_s Y_{lm}^* &= (-1)^{m+s} {}_{-s} Y_{l-m}, \\ \bar{\partial} {}_s Y_{lm} &= [(l-s)(l+s+1)]^{1/2} {}_{s+1} Y_{lm}, \\ \bar{\partial} {}_s Y_{lm} &= -[(l+s)(l-s+1)]^{1/2} {}_{s-1} Y_{lm}, \\ \bar{\partial} \bar{\partial} {}_s Y_{lm} &= -(l-s)(l+s+1) {}_s Y_{lm}. \end{aligned} \quad (16)$$

We now can expand the polarization (5) and its complex conjugate by the spin-2 spherical harmonics (15). We have

$$(Q \pm iU)(\hat{n}) = \sum_{lm} (E_{lm} \pm iB_{lm}) \pm 2 Y_{lm}(\hat{n}), \quad (17)$$

where the real and imaginary parts of the expansion components have been separated since  $Q$  and  $U$  are real parameters. With the help of the spin raising and lowering operators, together with Eqn (16),

we obtain

$$\begin{aligned}
\bar{\partial}^2(Q - iU)(\hat{n}) &= \sum_{lm} (E_{lm} - iB_{lm}) \bar{\partial} \bar{\partial} {}_{-2}Y_{lm}(\hat{n}) \\
&= \sum_{lm} (E_{lm} - iB_{lm}) \bar{\partial} (\sqrt{(l+2)(l-1)})^2 {}_{-1}Y_{lm}(\hat{n}) \\
&= \sum_{lm} \left[ \frac{(l+2)!}{(l-2)!} \right]^{1/2} (E_{lm} - iB_{lm}) Y_{lm}(\hat{n}), \\
\bar{\partial}^2(Q + iU)(\hat{n}) &= \sum_{lm} \left[ \frac{(l+2)!}{(l-2)!} \right]^{1/2} (E_{lm} + iB_{lm}) Y_{lm}(\hat{n}). \tag{18}
\end{aligned}$$

From these, the expansion coefficients can be found by using the orthonormality of spin-0 & -2 spherical harmonics:

$$\begin{aligned}
E_{lm} + iB_{lm} &= \int d\Omega {}_2Y_{lm}^*(\hat{n})(Q + iU)(\hat{n}) \\
&= \left[ \frac{(l-2)!}{(l+2)!} \right]^{1/2} \int d\Omega Y_{lm}^*(\hat{n}) \bar{\partial}^2(Q + iU)(\hat{n}), \\
E_{lm} - iB_{lm} &= \int d\Omega {}_{-2}Y_{lm}^*(\hat{n})(Q - iU)(\hat{n}) \\
&= \left[ \frac{(l-2)!}{(l+2)!} \right]^{1/2} \int d\Omega Y_{lm}^*(\hat{n}) \bar{\partial}^2(Q - iU)(\hat{n}). \tag{19}
\end{aligned}$$

From Eqns (19) it is clear that  $E_{lm}$  and  $B_{lm}$  are scalar spin-0 quantities. Furthermore, we can write these in the form

$$\begin{aligned}
E_{lm} &= \frac{1}{2} \left[ \frac{(l-2)!}{(l+2)!} \right]^{1/2} \int d\Omega Y_{lm}^*(\hat{n}) \left( \bar{\partial}^2(Q + iU)(\hat{n}) + \bar{\partial}^2(Q - iU)(\hat{n}) \right), \\
B_{lm} &= \frac{-i}{2} \left[ \frac{(l-2)!}{(l+2)!} \right]^{1/2} \int d\Omega Y_{lm}^*(\hat{n}) \left( \bar{\partial}^2(Q + iU)(\hat{n}) - \bar{\partial}^2(Q - iU)(\hat{n}) \right). \tag{20}
\end{aligned}$$

Using the above equations it is now easy to show that  $E_{lm}$  and  $B_{lm}$  have distinct parities. let us consider the space inversion where we reverse the sign of the  $x$ -coordinate, but leave the others unchanged. In spherical coordinates this amounts to  $r \rightarrow r$ ,  $\theta \rightarrow \theta$  and  $\phi \rightarrow \phi + \pi$  (therefore  $\partial_{\theta'} = \partial_{\theta}$  and  $\partial_{\phi'} = -\partial_{\phi}$ ). Let  $\hat{n} = (\theta, \phi)$  and  $\hat{n}' = (\theta', \phi')$  refer to the same physical direction in the original and space-inversed frames, respectively. From the definition of the Stokes parameters  $Q = \langle |\vec{\epsilon}_x|^2 \rangle - \langle |\vec{\epsilon}_y|^2 \rangle$ , and  $U = \langle \vec{\epsilon}_x \vec{\epsilon}_y^* \rangle + \langle \vec{\epsilon}_y \vec{\epsilon}_x^* \rangle$ , we therefore expect that under this transformation

$Q'(\hat{n}') = Q(\hat{n})$  and  $U'(\hat{n}') = -U(\hat{n})$ . So  $Q$  has even parity, while  $U$  has odd parity. Now using Eqns (11) and (12) and considering that  $(Q + iU)'(\hat{n}') = (Q - iU)(\hat{n})$ , we have

$$\begin{aligned}\bar{\partial}(Q + iU)'(\hat{n}') &= \frac{-1}{\sin^2 \theta'} \left( \partial_{\theta'} - \frac{i}{\sin \theta'} \partial_{\phi'} \right) \sin^2 \theta' (Q + iU)'(\hat{n}') \\ &= -\sin^{-2} \theta \left( \partial_{\theta} + \frac{i}{\sin \theta} \partial_{\phi} \right) \sin^2 \theta (Q - iU)(\hat{n}) \\ &= \bar{\partial}(Q - iU)(\hat{n})\end{aligned}\tag{21}$$

and likewise

$$\bar{\partial}^2(Q + iU)'(\hat{n}') = \bar{\partial}^2(Q - iU)(\hat{n})\tag{22}$$

Substituting Eqn (22) into (19), we will have  $E'_{lm}(\hat{n}') = E_{lm}(\hat{n})$  and  $B'_{lm}(\hat{n}') = -B_{lm}(\hat{n})$ . Therefore  $E$  and  $B$  have even and odd parities respectively. It is useful to define two quantities in real space

$$E(\hat{n}) = \sum_{lm} E_{lm} Y_{lm}(\hat{n})\tag{23}$$

$$B(\hat{n}) = \sum_{lm} B_{lm} Y_{lm}(\hat{n})\tag{24}$$

Under parity transformation the pattern of  $E(\hat{n})$  remains the same, while that of  $B(\hat{n})$  changes sign. Thus  $E$  and  $B$  can be thought of as the electric (i.e. ‘gradient’) and magnetic (i.e. ‘curl’) modes of the polarization function. Typical  $E$  or  $B$  type polarization patterns are shown in figure 4.

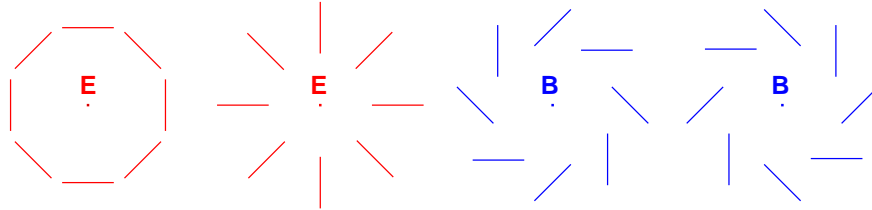


Figure 4: Typical  $E$  or  $B$  type polarization patterns. The electric and magnetic modes of the polarization are distinguished by their behavior under reflection.

To characterize the statistics of the CMB perturbations, we now define the power spectra. Since the primordial perturbations are expected to be Gaussian to a high degree of accuracy and since linear theory is the highly accurate approximation to the evolution of these perturbations until last

scattering, the small anisotropies of the temperature and polarization in the CMB are expected to follow Gaussian statistics. Therefore the expansion components in Eqns (1) and (17) each is an independent Gaussian deviate with

$$\langle T_{lm} \rangle = \langle E_{lm} \rangle = \langle B_{lm} \rangle = 0. \quad (25)$$

We now have three sets of multiple moments which fully describe the temperature and polarization map of the sky. Because of the Gaussianity of the anisotropies and because of the fact that anisotropies are so small that the universe is globally isotropic, all the information in the CMB perturbations can comprehensively be summarized in the power spectra of the perturbations. These are given by statistical isotropy which implies that

$$\begin{aligned} \langle T_{lm} T_{l'm'}^* \rangle &= \delta_{ll'} \delta_{mm'} \langle C_l^{TT} \rangle, \\ \langle T_{lm} E_{l'm'}^* \rangle &= \delta_{ll'} \delta_{mm'} \langle C_l^{TE} \rangle, \\ \langle E_{lm} E_{l'm'}^* \rangle &= \delta_{ll'} \delta_{mm'} \langle C_l^{EE} \rangle, \\ \langle B_{lm} B_{l'm'}^* \rangle &= \delta_{ll'} \delta_{mm'} \langle C_l^{BB} \rangle, \end{aligned} \quad (26)$$

where the power spectra  $\langle C_l \rangle \equiv C_l^{th}$  are specified by the theory of primordial perturbations. Here  $\delta$  is the Kronecker symbol and the angle brackets denote ensemble average over all realizations of the sky. The  $B$  pattern changes sign under parity transformation, so cross-correlations between  $B$  and  $T$  or  $E$  vanish ( $\langle B_{lm} E_{l'm'}^* \rangle = \langle B_{lm} T_{l'm'}^* \rangle = 0$ ). Simple statistical estimator of various  $C_l$ 's can be constructed from maps of the microwave background temperature and polarization. An unbiased estimator of the power spectra is given by

$$\begin{aligned} C_l^{TT} &= \frac{1}{2l+1} \sum_m \langle T_{lm} T_{l'm'}^* \rangle, \\ C_l^{TE} &= \frac{1}{2l+1} \sum_m \langle T_{lm} E_{l'm'}^* \rangle, \\ C_l^{EE} &= \frac{1}{2l+1} \sum_m \langle E_{lm} E_{l'm'}^* \rangle, \\ C_l^{BB} &= \frac{1}{2l+1} \sum_m \langle B_{lm} B_{l'm'}^* \rangle. \end{aligned} \quad (27)$$

These are  $\chi_\nu^2$ -distributed with the mean values equal to  $C_l^{th}$ ,  $\nu = 2l + 1$  degrees of freedom and a variance of  $2C_l^{th}/\nu$ .

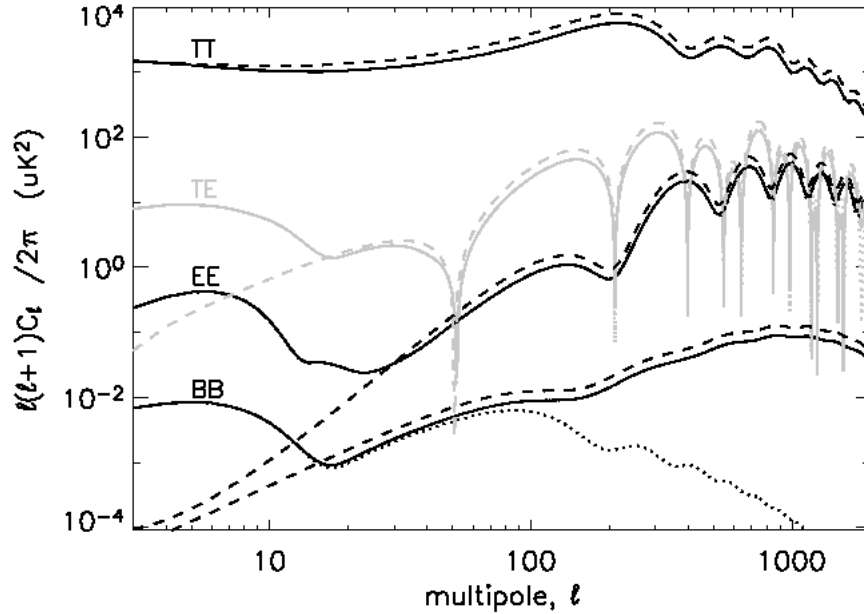


Figure 5: CMB temperature and polarization power spectra. The dashed lines are the spectra for a model with no re-ionization while the dotted lines are the spectra for a model with no gravitational lensing. The solid lines include the effect of both gravitational lensing and re-ionization.

Figure 5 shows the CMB power spectra decomposed into auto-correlation and cross-correlation of the temperature and polarization modes. The spectra have been generated by the CMBFAST code that is a Boltzmann and Einstein solver for the theory of cosmological perturbations. As we said earlier, the CMB polarization signal primarily arises from the Thomson scattering of the CMB photons during recombination. However, the polarization can also be altered after recombination by two processes before they can actually be detected. These are re-ionization and weak gravitational lensing of the cosmic microwave background. The effect of re-ionization which occurred when the first few generations of stars and quasars emitted radiation that reionized the universe was to increase the polarization signal on large scales. This leads to an increase in the amplitude of the polarization spectra on large scales ( $l \leq 20$ ) because the re-ionization had to happen and end at rather low redshifts ( $7 < z < 11.3$ ). On the other hand, weak lensing that is due to the deflection of CMB photons

by the gravitational potential of large scale structures affects polarization signals on small angular scales. Lensing converts some  $E$ -mode polarization into  $B$ -modes, that is to say there will be a scalar contribution to the  $B$ -mode spectrum on small scales due to lensing. However, for the  $TT$  and  $EE$  spectra, gravitational lensing results only in a smearing of the acoustic peaks on small scales, although the change to the spectra is very small. The lensing signal also contains useful information about large-scale structures which can be used to constrain cosmological parameters such as the neutrino mass. In figure 5 the spectra without gravitational lensing are shown by dotted lines while dashed lines are the spectra without re-ionization. The contribution to the spectra on large scales due to re-ionization and on small scales due to gravitation lensing are evident.

Furthermore, the decomposition of polarization field into the  $E$  and  $B$  modes can be useful to separate the gravitational waves (tensor) contribution from the density perturbation (scalar) contribution. This is because of the fact that different sources of temperature anisotropies give different patterns in the polarization. The CMB temperature fluctuations are the imprint of density and metric perturbations on the last scattering surface. They are classified as scalar ( $m = 0$ ), vector ( $m = \pm 1$ ) and tensor ( $m = \pm 2$ ) depending on their transformation properties under rotation. Scalar perturbations comprise total density fluctuations. Vector contributions get damped by expansion. Tensor fluctuations are expected from the primordial gravity waves predicted in the inflationary scenario. In their paper [3] Wayne Hu and Martin White show that the polarization pattern associated to each of these modes is different. The  $E$ -modes can be produced by both scalar and tensor perturbations, but the  $B$ -modes produced at last scattering can only be generated by tensor perturbations. Therefore, the relative amplitude of the  $BB$  polarization spectrum of the CMB is a constraint on the ratio of gravity waves to scalar perturbations, and thus give new information about inflationary parameters. These gravity wave signal peaks around scales of about  $l = 100$  in the spectrum of the  $B$ -mode polarization.

## APPENDIX A: Polarization From Thomson Scattering

Having described how polarization is generated by Thomson scattering, we now want to formulate these discussions and sum over all incident rays to derive statements for the  $Q$  and  $U$  components of the polarization for the outgoing scattered radiation. First, define the polarization vectors for the outgoing beam of light so that  $\hat{e}_1$  is perpendicular to the scattering plane and  $\hat{e}_2$  is in the scattering plane. (Figure 6) The Thomson scattering cross-section for an incident wave with linear polarization  $\hat{e}'$  into a scattered wave with linear polarization  $\hat{e}$  is given by

$$\frac{d\sigma}{d\Omega_{n'}} = \frac{3\sigma_T}{8\pi} |\hat{e}' \cdot \hat{e}|^2, \quad (28)$$

where  $\sigma_T$  is the total Thomson cross section and  $d\Omega_{n'}$  is the differential solid angle in the direction of the incoming ray  $\hat{n}'$ . Consider first an unpolarized incident plane wave of intensity  $I'$ , so  $Q' = U' = V' = 0$ . The  $Q$  polarization of the outgoing wave is the difference between the cross-section for photons polarized in the  $\hat{e}_1$  and  $\hat{e}_2$  directions. Hence, we have

$$Q = \frac{3\sigma_T}{8\pi} \left( \sum_{j=1}^2 |\hat{e}_1 \cdot \hat{e}'_j(\hat{n}')|^2 - \sum_{j=1}^2 |\hat{e}_2 \cdot \hat{e}'_j(\hat{n}')|^2 \right). \quad (29)$$

Without loss of generality, we can choose the  $\hat{z}$  axis to be along the propagation direction of the scattered light. So we can choose the two outgoing polarization axes as  $\hat{e}_1 = \hat{x}$  and  $\hat{e}_2 = \hat{y}$ . Integrating over all  $\hat{n}'$  directions, Eqn (29) leads to

$$Q(\hat{z}) = \int d\Omega_{n'} I'(\hat{n}') \sum_{j=1}^2 \left( |\hat{x} \cdot \hat{e}'_j(\hat{n}')|^2 - |\hat{y} \cdot \hat{e}'_j(\hat{n}')|^2 \right). \quad (30)$$

To take the dot product in Eqn (30), we express  $\hat{e}'_1$  and  $\hat{e}'_2$  in terms of their cartesian coordinates:

$$\hat{e}'_1(\theta', \phi') = (\cos \theta' \cos \phi', \cos \theta' \sin \phi', -\sin \theta'), \quad (31)$$

$$\hat{e}'_2(\theta', \phi') = (-\sin \phi', \cos \phi', 0). \quad (32)$$

Now, the dot products become trivial, and we find

$$\begin{aligned} Q(\hat{z}) &= \int d\Omega_{n'} I'(\hat{n}') \left[ (\cos^2 \theta' \cos^2 \phi' + \sin^2 \phi') - (\cos^2 \theta' \sin^2 \phi' - \cos^2 \phi') \right] \\ &= \int d\Omega_{n'} I'(\hat{n}') \left[ (\cos^2 \phi' - \sin^2 \phi') (\cos^2 \theta' - 1) \right] \\ &= - \int d\Omega_{n'} I'(\hat{n}') \sin^2 \theta' \cos(2\phi'). \end{aligned} \quad (33)$$

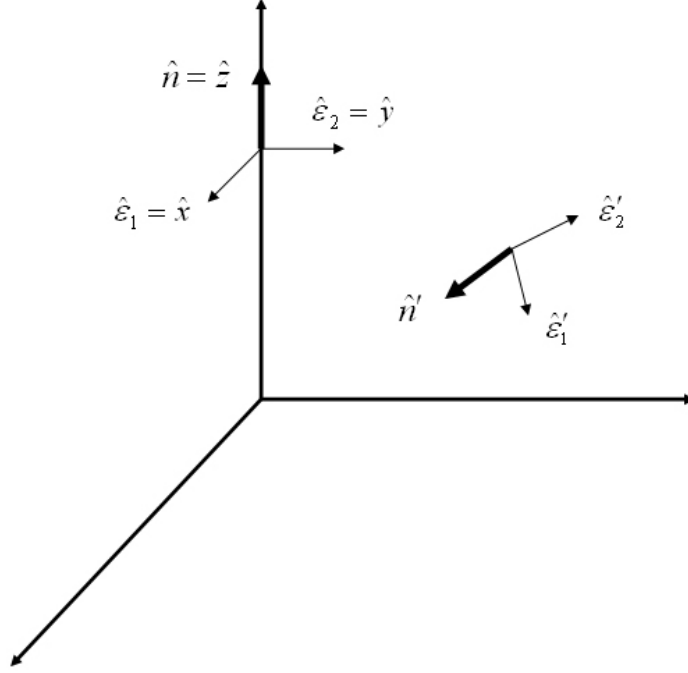


Figure 6: Incoming and outgoing polarization vectors for Thomson scattering of a light beam.

In the same way we can derive the corresponding expression for  $U(\hat{z})$ . The  $U$ -component of the polarization is proportional to the difference between the cross-section for outgoing photons polarized in the  $(\hat{x} + \hat{y})/\sqrt{2}$  and  $(\hat{x} - \hat{y})/\sqrt{2}$  directions. It is then straightforward to derive the  $U$ -component as follows

$$\begin{aligned}
U(\hat{z}) &= \int d\Omega_{n'} I'(\hat{n}') \sum_{j=1}^2 \left( \left| \left( \frac{\hat{x} + \hat{y}}{\sqrt{2}} \right) \cdot \hat{\epsilon}'_j(\hat{n}') \right|^2 - \left| \left( \frac{\hat{x} - \hat{y}}{\sqrt{2}} \right) \cdot \hat{\epsilon}'_j(\hat{n}') \right|^2 \right) \\
&= \frac{1}{2} \int d\Omega_{n'} I'(\hat{n}') \left[ |(\cos \theta' \cos \phi' + \cos \theta' \sin \phi')|^2 + |(-\sin \phi' + \cos \phi')|^2 \right. \\
&\quad \left. - |(\cos \theta' \cos \phi' - \cos \theta' \sin \phi')|^2 - |(-\sin \phi' - \cos \phi')|^2 \right] \\
&= \frac{1}{2} \int d\Omega_{n'} I'(\hat{n}') \left[ (\cos^2 \theta' - 1)(1 + \sin 2\phi') + (1 - \cos^2 \theta')(1 - \sin 2\phi') \right] \\
&= - \int d\Omega_{n'} I'(\hat{n}') \sin^2 \theta' \sin(2\phi'). \tag{34}
\end{aligned}$$

The polarization (5) in the direction  $\hat{z}$  will then have the form

$$Q(\hat{z}) - iU(\hat{z}) = -\frac{3\sigma_T}{8\pi} \int d\Omega_{n'} \sin^2 \theta' e^{2i\phi'} I'(\theta', \phi'). \quad (35)$$

We can further expand the incident intensity by spherical harmonics

$$I'(\theta', \phi') = \sum_{lm} a'_{lm} Y_{lm}(\theta', \phi'). \quad (36)$$

Using the orthonormality of the  $Y_{lm}$  and considering that the integrand in Eqn (35) is proportional to  $Y_{22}(\theta', \phi') = \sqrt{15/32\pi} e^{2i\phi'} \sin^2 \theta'$ , Eqns (35) and (36) lead to

$$(Q - iU)(\hat{z}) = \frac{3\sigma_T}{2\pi} \sqrt{\frac{2\pi}{15}} a'_{22}. \quad (37)$$

Thus, polarization is generated along the outgoing  $\hat{z}$ -axis provided that the  $a'_{22}$  quadrupole moment of the incoming radiation is non-zero. To determine the outgoing polarization in a direction making an angle  $\beta$  with the  $z$ -axis, the same incoming radiation  $I'(\hat{z})$  field must be expanded in the new coordinate system

$$I'(\hat{z}) = \tilde{I}'(\hat{n}_{rot}) = \sum_{lm} \tilde{a}'_{lm} Y_{lm}(\hat{n}_{rot}), \quad (38)$$

where tilde refers to the quantities in the frame  $\hat{n}_{rot} = R(\beta)\hat{z}$ . The rotated multipole coefficients are

$$\begin{aligned} \tilde{a}'_{lm} &= \int d\hat{n}_{rot} Y_{lm}^*(\hat{n}_{rot}) \tilde{I}'(\hat{n}) \\ &= \int d(R(\beta)\hat{z}) Y_{lm}^*(R(\beta)\hat{z}) Y_{lm}^*(R(\beta)\hat{z}) I'(\hat{z}) \\ &= \sum_{m'=-m}^m \mathcal{D}_{m'm}^{l*}(R(\beta)) \int d\hat{z} Y_{lm'}^*(\hat{z}) I'(\hat{z}) \\ &= \sum_{m'=-m}^m \mathcal{D}_{mm'}^{l*}(R(\beta)) a'_{lm'}, \end{aligned} \quad (39)$$

where  $\mathcal{D}_{mm'}^l$  is the Wigner D-symbol. We see that only  $a'_{2m}$  components of incident radiation contribute to  $\tilde{a}'_{22}$  which generates the polarization in the  $\hat{n}_{rot}$  direction. Hence the polarization in the new direction is

$$(Q - iU)(\hat{n}_{rot}) = \frac{3\sigma_T}{2\pi} \sqrt{\frac{2\pi}{15}} \sum_{m=-2}^2 \mathcal{D}_{2m}^{2*}(R(\beta)) a'_{2m}. \quad (40)$$

Thus, the total scattered radiation in any direction of sky is polarized only if there exists a nonzero quadrupole moment in the incident radiation field. For the case when the incoming radiation field is independent of  $\phi'$  only the  $a'_{20}$  component of the quadrupole is nonzero, then  $\tilde{a}'_{22} = a'_{20} \mathcal{D}_{02}^{2*}(R) \equiv a'_{20} d_{02}^{2*}(\beta) = \sqrt{6}/4 a'_{20} \sin^2 \beta$ . Hence

$$(Q - iU)(\hat{n}_{rot}) = \frac{3\sigma_T}{4\pi} \sqrt{\frac{\pi}{5}} a'_{20} \sin^2 \beta. \quad (41)$$

Since the incoming field is real,  $a'_{20}$  will be real, and  $U = 0$ . Hence, an azimuthally symmetric field will generate a polarized scattered field which is oriented in the plane of the  $z$ -axis and the scattering direction. The magnitude of polarization is maximal along the equator where  $\beta = \pi/2$ . In this way, the contribution from different  $a'_{2m}$  quadrupole modes of the incident field to the  $Q$  and  $U$  varies depending on our line of sight.

## References

- [1] M. Bowden et al. (2004), astro-ph/0309610.
- [2] S. Dodelson, Modern Cosmology (Academic Press, 2003).
- [3] W. Hu, M. White (1997), astro-ph/9706147.
- [4] J. Kaplan, J. Delabrouille, P. Fosalba, C. Rosset (2005), astro-ph/0310650.
- [5] A. Kosowsky (1999), astro-ph/9904102.
- [6] A. Kosowsky (1995), astro-ph/9501045.
- [7] Y.T. Lin, B.D. Wandelt (2004), astro-ph/0409734.